Organic & Biomolecular Chemistry

ROYAL SOCIETY OF CHEMISTRY

COMMUNICATION

View Article Online
View Journal | View Issue

Cite this: *Org. Biomol. Chem.*, 2021, **19**, 2192

Received 16th November 2020,
Accepted 16th February 2021

DOI: 10.1039/d0ob02277b

rsc.li/obc

A powerful azomethine ylide route mediated by TiO_2 photocatalysis for the preparation of polysubstituted imidazolidines†

Anan Liu,[a,c] Dongge Ma,*[b] Yuhang Qian,[b] Jundan Li,[b] Shan Zhai,[b] Yi Wang[b] and Chuncheng Chen[d]

Lewis- and Brønsted-acid catalyzed 1,3-dipolar cycloaddition between azomethine ylides and unsaturated compounds is an important strategy to construct five-membered N-heterocycles. However, such a catalytic route usually demands substrates with an electron-withdrawing group (EWG) to facilitate the reactivity. Herein, we report a TiO_2 photocatalysis strategy that can conveniently prepare five-membered N-heterocyclic imidazolidines from a common imine (*N*-benzylidenebenzylamine) and alcohols along the route of 1,3-dipolaron azomethine ylide but without pre-installed EWG substituents on the substrates. Our EPR results uncovered the previously unknown mutual interdependence between an azomethine ylide and TiO_2 photo-induced h_{vb}^+/e_{cb}^- pair. This transformation exhibited a broad scope with 21 successful examples and could be scaled up to the gram level.

Lewis- and Brønsted-acid catalyzed 1,3-dipolar cycloaddition between azomethine ylides and imines, *i.e.*, Hüisgen reaction, is one of the most important methods to prepare various N-heterocyclic molecules for natural products, pharmaceuticals, pesticides and fine chemicals.[1] Perfect regioselectivity and diastereoselectivity or enantioselectivity have been achieved by such designable azomethine ylide strategies. However, the substrate scope is mostly limited to azomethine ylides with an electron-withdrawing group (EWG) adjacent to their carbanion center[2] so far (see Scheme 1a, the right-hand side). There are sparse successful reports that focused on 1,3-dipolar cycloaddition through an unstabilized azomethine ylide catalyzed by diphenylphosphate. However, in these cases, it is still required that another substrate, dipolarophile imines, must have strong EWGs such as nosyl and tosyl groups to make the reaction proceed smoothly.[3] Therefore, developing methods that can accommodate common azomethine ylides and imines without pre-installed stabilizing EWGs is in urgent need, especially for the preparation of polysubstituted imidazolidine compounds.[4]

Photoredox catalysis for the purposes of organic transformation has experienced a resurgence in the past decades.[5] Compared with the mainstream noble metal Ru- and Ir-based homogeneous photocatalysts,[6] Earth-abundant and non-toxic TiO_2 nanomaterials emerged relatively late in the organic chemists' toolbox. TiO_2-based photocatalysis potential from the aspect of organic synthetic chemistry has only been revisited recently.[7–13] There have been some examples in the application of photo-induced h_{vb}^+/e_{cb}^- on the TiO_2 surface to realize single- or two-electron transfer redox reactions.[14–25] Nonetheless, TiO_2 photocatalysis based on the single-electron-transfer (SET) or free-radical mechanism is seldom used in more common acid/base catalytic reactions, although these reactions actually have wider application scopes in organic synthesis by means of nucleophilic and electrophilic reactivity. TiO_2 photocatalysts themselves, in terms of thermal catalysis, were not believed to possess either Lewis or Brønsted acid/base catalytic activity (pI = 6.8) at room temperature. Very recently, we found that the photo-induced protons from alcohol oxidation on the TiO_2 surface possess strong Brønsted-acid properties owing to the co-existent weakest conjugated base, *i.e.*, the delocalized conduction-band electron (e_{cb}^-) acts as a conjugated Brønsted base.[26] This photocatalytic pathway enables a non-trivial aromatic electrophilic substitution reaction coupled with photo-induced e_{cb}^-. Herein, we report another unrevealed function of the photo-induced h_{vb}^+/e_{cb}^- pair that can catalytically transform an enamine intermediate

[a]*Basic Experimental Centre for Natural Science, University of Science and Technology Beijing, 30 Xueyuan Road, Beijing, 100083, China*
[b]*Department of Chemistry, College of Chemistry and Materials Engineering, Beijing Technology and Business University, Fucheng Road 11, Beijing, 100048, China. E-mail: madongge@btbu.edu.cn*
[c]*School of Chemistry and Biological Engineering, University of Science and Technology Beijing, 30 Xueyuan Road, Beijing, 100083, China*
[d]*Key Laboratory of Photochemistry, Institute of Chemistry, Chinese Academy of Sciences, Zhongguancun North First Street 2, Beijing, 100190, China*

†Electronic supplementary information (ESI) available. CCDC 1856874. For ESI and crystallographic data in CIF or other electronic format see DOI: 10.1039/d0ob02277b

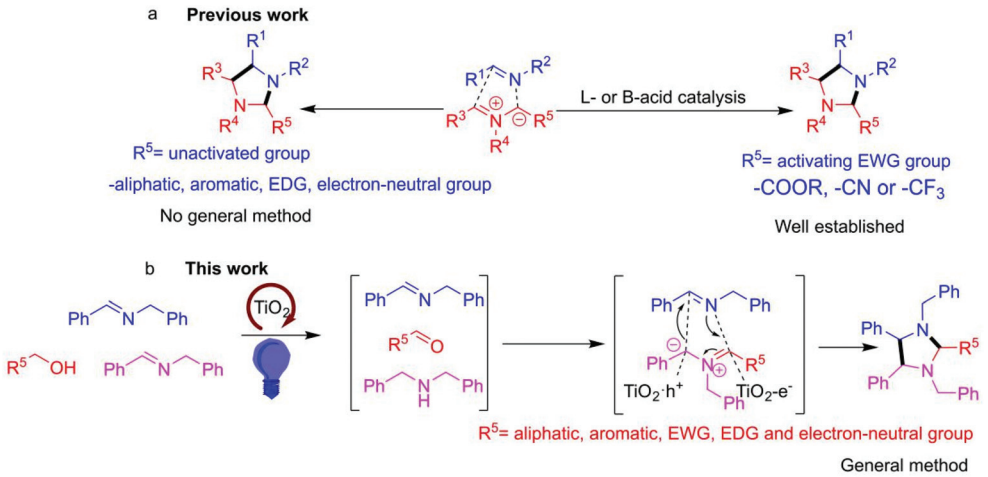

Scheme 1 1,3-Dipolar cycloaddition to synthesize imidazolidines through the azomethine ylide intermediate.

into highly active azomethine ylide species, and these substrates without pre-installed EWGs are readily used for 1,3-dipolar cycloaddition reactions (Scheme 1b). This reactivity is unprecedented in conventional Lewis and Brønsted acid/base thermal catalytic reactions.

Based on our group's constant research in TiO_2-based photocatalysis applied in organic synthesis,[10–13,20,23,25] we envisioned a possible reaction route for this transformation (as shown in Scheme 2). We selected common imines and alcohols as remote precursors of azomethine ylide in place of enamines that traditionally must have necessary EWG substituents. Under photoirradiation, the TiO_2 photocatalyst may transform imine and alcohol into an active enamine intermediate *via* the condensation of nascent aldehyde and amine delivered from photo-induced h_{vb}^+/e_{cb}^-, respectively (eqn (2)–(4) in Scheme 2). An azomethine ylide species was in tandem generated by another photo-induced h_{vb}^+/e_{cb}^-, in which photo-induced h_{vb}^+/e_{cb}^- did not act as a conventional redox agent but as a Lewis acid/base to catalyze the formation of azomethine ylide from *in situ* formed enamine (eqn (5) in Scheme 2). The as-formed azomethine ylide would be reactive to result in sequential 1,3-dipolar cycloaddition with excess dipolarophile imine (eqn (6) in Scheme 2). Alcohols used here, on the one hand, significantly expand the scope of enamines by the introduction of alternative R^5 groups (see Scheme 1b). On the other hand, they generally have overwhelming reactivity greater than those of other substrates and intermediates to avoid being over-oxidized by active photo-induced h_{vb}^+. In this way, a series of pharmaceutically important polysubstituted 1,3-dibenzylimidazolidine molecules[27] could be produced from commercially available alcohols and imines (Scheme 1b). In contrast, traditional Lewis- or Brønsted-acid and noble metal-based catalysis always requires activating EWG substituents in either azomethine ylide or imine (Scheme 1a).

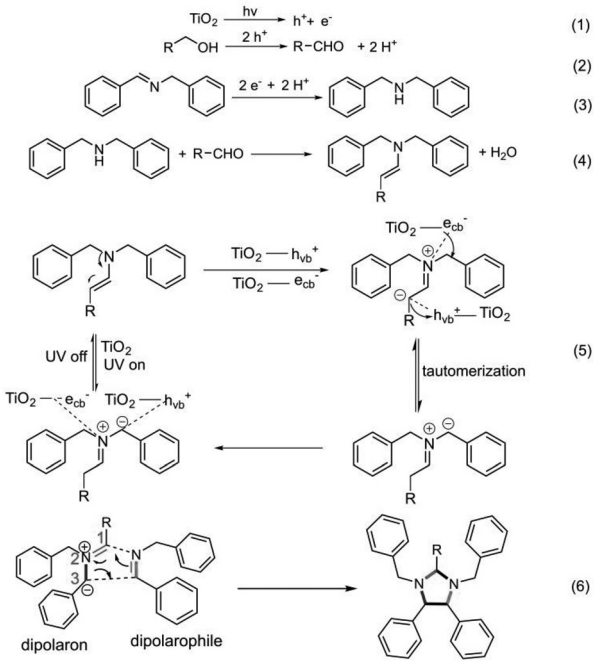

Scheme 2 Proposed route of TiO_2 photocatalyzed 1,3-dipolar cycloaddition between NBBA and alcohols.

Using *N*-benzylidenebenzylamine (NBBA) and ethanol as the model substrates, ethanol itself as the solvent and P25 TiO_2 as the photocatalyst under an anaerobic Ar atmosphere, the aimed imidazolidine product with almost quantitative 98% yield was dramatically produced under 300 W Xe lamp irradiation. The product structure was confirmed by X-ray single-crystal diffraction, ^{1}H-NMR, ^{13}C-NMR and HR-ESI-MS characterization techniques (see ESI sections VII, IX, and X and CCDC-1856874.cif†). A number of control and optimization experiments were conducted to screen the optimum conditions. The results are shown in Table 1 and Tables S1–S3.† Both UV irradiation and the TiO_2 photocatalyst were the prerequisites for successful transformation (see Table S1†). Other visible-light responsive photocatalysts could not provide the

Table 1 Control and optimization of TiO_2 photocatalytic 1,3-dipolar cycloaddition between NBBA and ethanol

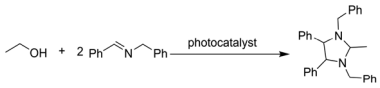

Entry	Photocatalyst	Irradiation	Atmosphere	Yield[a] (%)
1	P25 TiO_2	Yes	Ar	98
2	None	Yes	Ar	8
3	P25 TiO_2	No	Ar	ND
4	P25 TiO_2	Yes	N_2	85
5	P25 TiO_2	Yes	O_2	Trace
6	P25 TiO_2	Yes	Air	Trace
7[b]	P25 TiO_2	Yes	Ar	91[c]

Reaction conditions: 1 mmol NBBA, 32 mg P25 TiO_2, 3 mL ethanol, 300 W Xe lamp, 5 h. [a] GC yield. [b] For the gram scale synthesis: NBBA, 7.6 mmol; P25 TiO_2, 80 mg; ethanol, 10 mL; 300 W Xe lamp; 48 h. [c] Isolated yield.

aimed imidazolidine product (see Table S2†). Changing the atmosphere to 1 atm O_2 or air led to only a trace amount of the product, indicating the necessity of an anaerobic atmosphere (see Table 1). Furthermore, the transformation could be scaled up to the gram level, providing a nearly unreduced isolated yield of 91% with 1.17 g aimed product after column purification (see ESI section VI†). The TiO_2 photocatalyst after several recycles and reuse still retained high activity. By simple centrifugation and washing of the catalyst after each use, an almost undiminished yield of 95% after 5 cycles was achieved (Fig. S1†). Until now, the P25 TiO_2 photocatalyst did not experience an apparent morphology change (Fig. S2†). As shown in Table S3,† changing the solvent from ethanol to MeCN led to a decrease in the yield from 98% to 75%. Other polar aprotic solvents such as DMF and DMSO also showed further decreased yields (45% and 38%, respectively). When non-polar solvents toluene and *n*-hexane were used, much lower yields were obtained. The dependence of the yield on the solvent polarity suggested that the photocatalytic reaction probably proceeds through a charged intermediate (the most probable being azomethine ylide) rather than a neutral radical intermediate. With the optimized conditions in hand, we began to explore the scope of substrate alcohols. Short-chain primary alcohols provided excellent yields (see Fig. 1; **1a**, **1b**, and **1c**), while long-chain alcohols such as *n*-butanol and *n*-octanol (see Fig. 1; **1d** and **1e**) also achieved fair yields. Branched primary alcohols (**1f** and **1g**) provided moderate yields. This method was also suitable for aromatic primary alcohols, but the solvent should be changed from neat alcohol to MeCN (Table S3†). Benzyl alcohol and 4-methyl and 2-methylbenzyl (**1h**, **1i**, and **1j**) alcohols were all feasible substrates. Electron-rich 4-methoxyl and 4-*N*,*N*′-dimethylamino benzyl alcohols provided moderate to good yields (**1k** and **1l**). Compared with electron-rich alcohols, electron-poor alcohols gave lower yields. 4-Trifluoromethyl, 4-cyano, 4-F, 4-Cl, 4-Br and 4-methyl benzoate substituted benzyl alcohols (**1m**, **1n**, **1o**, **1p**, **1q**, and **1r**) showed moderate but synthetically useful yields. This method could be extended

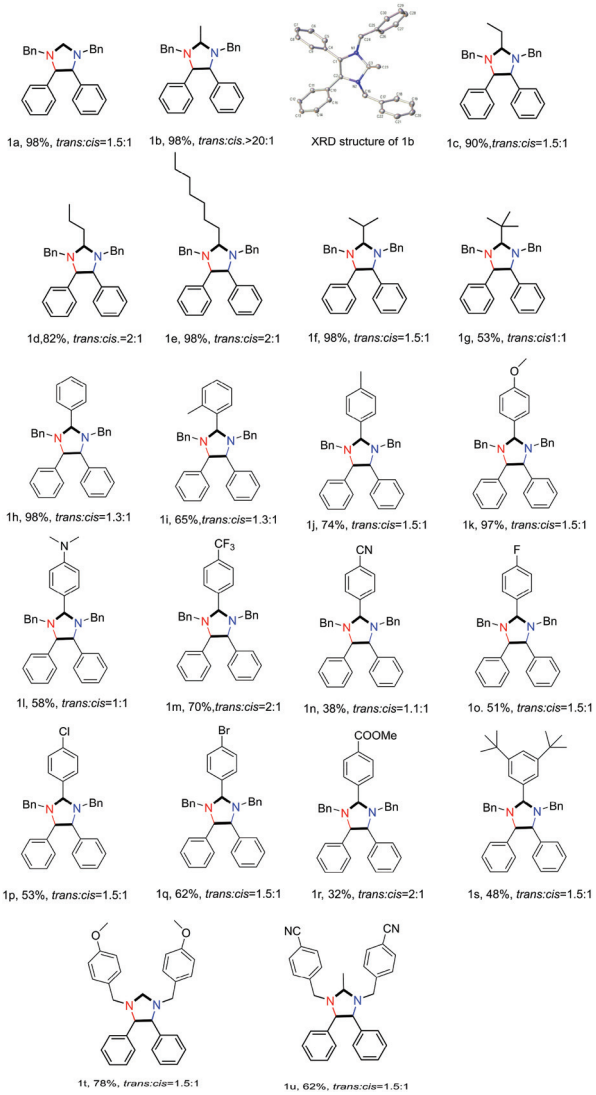

Fig. 1 TiO_2 photocatalytic 1,3-dipolar cycloaddition between different alcohols and imines.

to sterically crowded 3,5-di-*tert*-butyl benzyl alcohol (**1s**). To broaden the substrate scope of this photocatalytic method, we changed another reactant NBBA with EWG and EDG substituents at the *para*-position of its benzylamine ring (**1t** and **1u**, respectively). As a result, both cases showed very satisfactory yields (78% for **1t** and 62% for **1u**) and supported the validity of this strategy. In addition, since the two phenyl groups linked to the *C*4 and *C*5 positions of the imidazolidine product generally resulted in a diastereoisomeric mixture of two couples (*i.e.*, *trans*-4*S*,5*S* and -4*R*,5*R*; *cis*-4*S*,5*R* and -4*R*,5*S*), the relative configuration of each diastereoisomer was determined through comparing the tendency of chemical shifts in the ^{1}H-NMR spectra of each couple diastereomers and their coupling patterns with those of **1b** since **1b** was obtained as an almost single isomer and its XRD structure showed the *trans*-configuration (see ESI section X†). Fig. 1 shows the ratios of the *trans*- : *cis*-configuration of every product. Most of the ratios

of *trans*- to *cis*- were in the range of 2 : 1 ~ 1 : 1, except for **1b**, indicating that this pathway had little diastereoselectivity.

To further demonstrate the significance of this method, we conducted the 1,3-dipolar cycloaddition experiments of either the unactivated or the activated azomethine ylide precursor to compare TiO_2 photocatalysis with typical Lewis-[1,28] and Brønsted-acid[3,29] catalysis. As shown in Table 2, when exposed to the TiO_2 photocatalysis system, the azomethine ylide precursor imines bearing either unactivated phenyl as eqn (7) (entry 1 in Table 2) or the activated EWG ester group as eqn (8) (entry 11 in Table 2) reacted with ethanol to form the imidazolidine product in almost perfect quantitative yield (~95% and ~92%, respectively). However, when the azomethine ylide precursor imine NBBA with the unactivated phenyl group was applied under either typical Lewis-acid (AgOAc (entries 2 and 3 in Table 2) and $Cu(CH_3CN)_4BF_4$ (entries 5 and 6 in Table 2)) or Brønsted-acid (DPP) (entries 8 and 9 in Table 2) catalysis conditions, no aimed cycloaddition product was observed using either ethanol or previously reported successful THF or DCM as the solvent.[28,29] Instead, using imines with the activated EWG ester group as eqn. (8) in Table 2, we obtained almost the same yield as reported in the literature under Lewis-acid AgOAc (entry 4) and $Cu(CH_3CN)_4BF_4$ (entry 7) or Brønsted-acid DPP (entry 10) catalysis conditions.[1,28,29] The control experiments shown in Table 2 adequately demonstrated that the 1,3-dipolar cycloaddition of imines both without (entry 1 in Table 2) and with the activated group such as the –COOMe group (entry 11 in Table 2) can be carried out smoothly by our TiO_2 photocatalysis strategy. TiO_2 photocatalysis exhibit powerful Lewis-acid catalytic activity besides its common photoredox property.

Table 2 Comparison of TiO_2 photocatalysis with Lewis/Brønsted acid catalysis in 1,3-dipolar cycloaddition of imine and the azomethine ylide precursor with either an stabilizing EWG (eqn. (8)) or an electron-neutral group (eqn. (7))

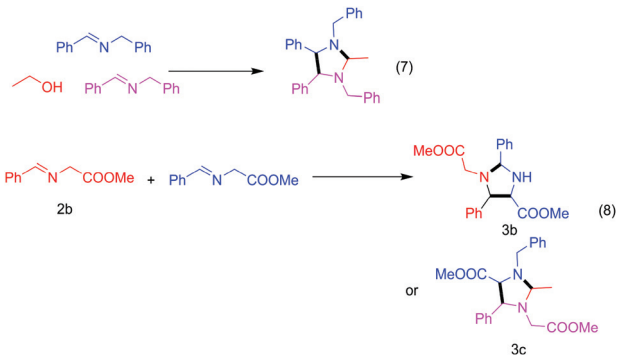

Entry	Catalyst	Eq.	Solvent	Conv. (%)	Yield[b] (%)
1[a]	P25 TiO_2	7	Ethanol	100	95
2[c]	AgOAc	7	Ethanol	5	ND
3[c]	AgOAc	7	THF	73	~0
4[c]	AgOAc	8	THF	100	94 (3b)
5[d]	$Cu(CH_3CN)_4BF_4$	7	Ethanol	48	~0
6[d]	$Cu(CH_3CN)_4BF_4$	7	DCM	28	~0
7[d]	$Cu(CH_3CN)_4BF_4$	8	DCM	100	95 (3b)
8[e]	DPP	7	Ethanol	98	~0
9[e]	DPP	7	DCM	99	~0
10[e]	DPP	8	DCM	99	93 (3b)
11[f]	P25 TiO_2	8	MeCN/EtOH	100	92 (3c)

[a] Reaction conditions: 1 mmol NBBA, 32 mg P25 TiO_2, 3 mL ethanol, 300 W Xe lamp illumination for 5 h at 5 cm distance. [b] Conversion and yield are based on ^{1}H-NMR with 1,3,5-trimethoxybenzene as the internal standard. [c] 5 mol% catalyst. [d] 3 mol% catalyst and 20 mol% Et_3N additive. [e] 20 mol% catalyst. Lewis-acid and Brønsted-acid catalyses were conducted strictly according to the literature for 1,3-dipolar cycloaddition between the azomethine ylide precursor with stabilizing EWGs and imines. [f] Reaction conditions as [a] but with 20% ethanol/MeCN as the cosolvent; its product was **3c**. Its characterization and NMR data are listed in the ESI.†

To shed light on the cascade reaction of the azomethine ylide precursor imine and alcohol assisted by TiO_2 photocatalysis, off-line GC-MS tracing experiments were performed. From the experimental results shown in Fig. 2, two key intermediates were identified. Dibenzylamine with m/z = 197 and *N*,*N*′-dibenzylethenamine with m/z = 223 were confirmed by GC-MS analysis against irradiation times.

Dibenzylamine is generated from the reduction of NBBA imine by photo-induced e_{cb}^- (eqn (3) in Scheme 2), while photo-induced h_{vb}^+ oxidizes primary alcohol to aldehyde (see Scheme 2, eqn (2) and (3)). The *N*,*N*′-dibenzylethenamine intermediate is generated from the consecutive condensation between dibenzylamine and aldehyde (see Scheme 2, eqn (4)). The observations of these two crucial intermediates were in excellent agreement with the proposed process of the 1,3-dipolar cycloaddition reaction in Scheme 2.

To demonstrate that the azomethine ylide intermediate was generated in the cascade reaction along the reaction pathway: alcohol oxidation to acetaldehyde and imine reduction to amine catalyzed by photo-induced h_{vb}^+/e_{cb}^-, respectively (eqn (2) and (3) in Scheme 2), we conducted the control experiments starting with dibenzylamine, NBBA imine and acetaldehyde instead of alcohol. As shown in Table 3, in the absence of either TiO_2 (entry 2) or irradiation (entry 3), the aimed cycloadduct product was not detected, while only a small amount of the condensation product enamine was obtained. Instead, under TiO_2 photocatalysis conditions, the aimed imidazolidine product could be obtained with a high yield (entry 1). This definitely showed that the 1,3-dipolar

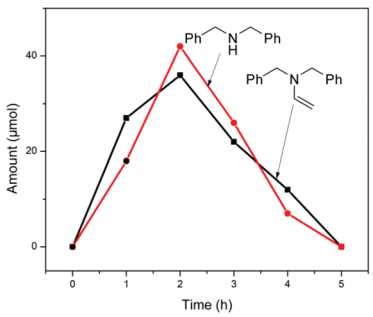

Fig. 2 Key intermediate formation and depletion against the reaction time. The red line represents dibenzylamine and the black line represents *N*,*N*′-dibenzylethenamine.

Table 3 Control experiments for the TiO_2 photocatalytic synthesis of imidazolidine from intermediates acetaldehyde, dibenzylamine and NBBA

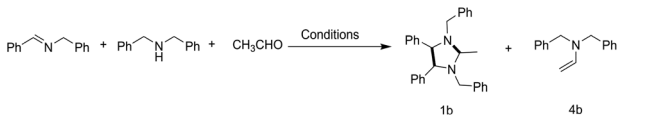

Entry	Catalyst	Irradiation	Yield[a] (%) (**1b**, **4b**)
1	P25 TiO_2	Yes	85, 4
2	None	Yes	14, 70
3[b]	P25 TiO_2	None	5, 72

Reaction conditions: 1 mmol dibenzylamine, 1 mmol NBBA, 1 mmol acetaldehyde, 3 mL anhydrous acetonitrile as the solvent, 32 mg P25 TiO_2, Ar atmosphere, under 300 W Xe lamp illumination for 8 hours at 5 cm distance. [a] GC yield. [b] Heating at 40 °C.

cycloaddition mechanism, if it was true, must be a photocatalyzed process. In other words, in this case, the photo-induced h_{vb}^+/e_{cb}^- pair neither plays a redox role nor promotes the condensation of aldehyde and amine into enamine; it plays a totally novel role to generate and stabilize the azomethine ylide intermediate for the 1,3-dipolar cycloaddition (as proposed in eqn (5) and (6) in Scheme 2).

As the key azomethine ylide species either with or without EWG groups is too transient to detect by off-line GC-MS or NMR analysis, alternatively, we sought to exploit the low-temperature 90 K electron paramagnetic resonance (EPR) technique to *in situ* characterize the other key species in the photocatalysis reaction, *i.e.*, photo-induced h_{vb}^+ and e_{cb}^-. Traditionally, due to the competing fast recombination processes between photo-induced h_{vb}^+ and e_{cb}^- species, it is necessary to add hole or electron sacrificial reagents to quench one of them to lengthen the lifetime of the other species for observations by EPR.[9,14] As proposed above, in this case, TiO_2 photo-induced h_{vb}^+/e_{cb}^- may also play a different role from the conventional redox view. Besides alcohol oxidation to aldehyde by photo-induced h_{vb}^+ and imine reduction to amine by photo-induced e_{cb}^- (see Scheme 2, eqn (2) and (3)), we argued that photo-induced h_{vb}^+/e_{cb}^- facilitates and stabilizes the azomethine ylide intermediate and thereby shows different EPR features. We took acetaldehyde, dibenzylamine and NBBA as substrates to perform the photocatalysis reaction in P25 TiO_2 suspension under UV irradiation as the case of entry 1 in Table 3 (that proceeded successfully to obtain the aimed imidazolidine product **1b**), in which we observed the *in situ* EPR signals of h_{vb}^+ and e_{cb}^- (see Fig. 3, top). Upon increasing the concentration of dibenzylamine, acetaldehyde and NBBA from 0.005 M to 0.1 M, we observed the gradual enhancement of both photo-induced h_{vb}^+ signals corresponding to g_1 = 2.014, g_2 = 2.011, and g_3 = 2.003 and photo-induced e_{cb}^- signals corresponding to g = 1.990, g = 1.982 and g = 1.945 together (Fig. 3, top). Such simultaneous occurrence and enhancement of photo-induced h_{vb}^+/e_{cb}^- signals in our experiment are rather unexpected and significantly different from nearly all photocatalytic events

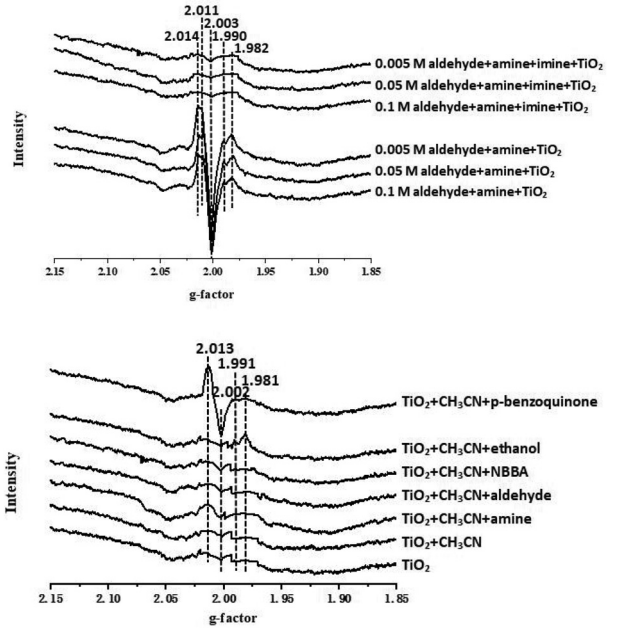

Fig. 3 (Top) EPR spectra measured at 90 K of P25 TiO_2 under UV irradiation in the CH_3CN solution of acetaldehyde and amine (0.005 M, 0.05 M and 0.1 M) and of acetaldehyde, amine and NBBA (0.005 M, 0.05 M and 0.1 M). (Bottom) Controlled ESR spectra measured at 90 K under UV irradiation of P25 TiO_2; P25 + CH_3CN; P25 + CH_3CN + dibenzylamine; P25 + CH_3CN + acetaldehyde; P25 + CH_3CN + NBBA; P25 + CH_3CN + ethanol; and P25 + CH_3CN + *p*-benzoquinone (1 ml CH_3CN; the organic substrate concentration is 0.1 M).

before.[30] Generally, the photo-induced h_{vb}^+ signal appears only when photo-induced e_{cb}^- is eliminated by the e_{cb}^- scavenger such as dioxygen,[31] or the signal of photo-induced e_{cb}^- appears only when the h_{vb}^+ scavenger such as alcohols is present.[23,32] Both species cannot be observed simultaneously in the EPR determination (at 90 K) because of the fast recombination between each other. The co-existence and enhancement of EPR signals of photo-induced h_{vb}^+ and e_{cb}^- together in our system have to be attributed to the stabilizing effect of photo-induced h_{vb}^+/e_{cb}^- species by azomethine ylide formation as shown in Scheme 2. It should be noted that in the absence of NBBA, the signals of both photo-induced h_{vb}^+ and e_{cb}^- dramatically decreased in comparison with those in the presence of NBBA under otherwise identical conditions (Fig. 3, top). That is, in the absence of dipolarophile imine, the formed enamine would not be smoothly converted into the final imidazolidine product through the azomethine ylide intermediate (as shown in Scheme 2, eqn (5) and (6)). At this moment, no appearance of h_{vb}^+ and e_{cb}^- signals somewhat suggested the relation of interdependence between azomethine ylide and photo-induced h_{vb}^+/e_{cb}^-. To further verify the unusual h_{vb}^+ and e_{cb}^- co-existence and enhancement together, we carried out a series of controlled EPR experiments (Fig. 3, bottom). As expected, only the photo-induced e_{cb}^- signal appeared when we added ethanol in the photocatalysis system to eliminate photo-induced h_{vb}^+, while we observed only the photo-induced

h_{vb}^+ signal when we added *p*-benzoquinone to eliminate photo-induced e_{cb}^-. More certainly, when there were no scavengers available to eliminate either photo-induced h_{vb}^+ or e_{cb}^-, we indeed did not observe any obvious EPR signals attributed to h_{vb}^+ or e_{cb}^-. Thus, our EPR results indicated that an interaction exists between azomethine ylide and TiO_2 photo-induced h_{vb}^+/e_{cb}^- species. A portion of TiO_2 photo-induced h_{vb}^+/e_{cb}^- species acts as the redox agent and the other part acts as the Lewis acid/base catalyst to dictate the high yields of 1,3-dipolar cycloaddition reactions. To the best of our knowledge, this is the first time that such a unique activity in TiO_2 photocatalysis is revealed.

In summary, we have demonstrated that as a cheap, stable, Earth-abundant and non-toxic heterogeneous photocatalyst, P25 TiO_2, could realize challenging non-activated 1,3-dipolar cycloaddition for the preparation of polysubstituted imidazolidines without numerous traditional auxiliaries and ligands. This method demonstrated a fairly broad substrate scope and functional group tolerance. More importantly, it is revealed for the first time that radically different from its well-known common redox transformation, the TiO_2 photocatalyst can also act as a powerful Lewis- and Brønsted-acid/base catalyst to realize important 1,3-dipolar cycloadditions without additional EWGs in substrates.

Conflicts of interest

There are no conflicts to declare.

Notes and references

1 H. Xie, J. Zhu, Z. Chen, S. Li and Y. Wu, *J. Org. Chem.*, 2010, **75**, 7468–7471.
2 Y. Saima, S. Khamarui, K. S. Gayen, P. Pandit and D. K. Maiti, *Chem. Commun.*, 2012, **48**, 6601–6603.
3 C. Izquierdo, F. Esteban, J. L. G. Ruano, A. Fraile and J. Alemán, *Org. Lett.*, 2016, **18**, 92–95.
4 R. Xu, R. Xia, M. Luo, X. Xu, J. Cheng, X. Shao and Z. Li, *J. Agric. Food Chem.*, 2014, **62**, 381–390.
5 F. Parrino, M. Bellardita, E. I. García-López, G. Marcì, V. Loddo and L. Palmisano, *ACS Catal.*, 2018, **8**, 11191–11225.
6 C. K. Prier, D. A. Rankic and D. W. C. MacMillan, *Chem. Rev.*, 2013, **113**, 5322–5363.
7 G. Palmisano, E. Garcia-Lopez, G. Marci, V. Loddo, S. Yurdakal, V. Augugliaro and L. Palmisano, *Chem. Commun.*, 2010, **46**, 7074–7089.
8 L. Palmisano, V. Augugliaro, M. Bellardita, A. Di Paola, E. G. Lopez, V. Loddo, G. Marci, G. Palmisano and S. Yurdakal, *ChemSusChem*, 2011, **4**, 1431–1438.
9 H. Kisch, *Angew. Chem., Int. Ed.*, 2013, **52**, 812–847.
10 D. Ma, A. Liu, S. Li, C. Lu and C. Chen, *Catal. Sci. Technol.*, 2018, **8**, 2030–2045.
11 Y. Wang, A. Liu, D. Ma, S. Li, C. Lu, T. Li and C. Chen, *Catalysts*, 2018, **8**, 355.
12 D. Ma, S. Zhai, Y. Wang, A. Liu and C. Chen, *Molecules*, 2019, **24**, 330.
13 D. Ma, S. Zhai, Y. Wang, A. Liu and C. Chen, *Front. Chem.*, 2019, **7**, 636.
14 A. L. Linsebigler, G. Lu and J. T. Yates, *Chem. Rev.*, 1995, **95**, 735–758.
15 S. Yurdakal, G. Palmisano, V. Loddo, V. Augugliaro and L. Palmisano, *J. Am. Chem. Soc.*, 2008, **130**, 1568–1569.
16 S. Füldner, R. Mild, H. I. Siegmund, J. A. Schroeder, M. Gruber and B. König, *Green Chem.*, 2010, **12**, 400–406.
17 M. Cherevatskaya, M. Neumann, S. Fueldner, C. Harlander, S. Kuemmel, S. Dankesreiter, A. Pfitzner, K. Zeitler and B. Koenig, *Angew. Chem., Int. Ed.*, 2012, **51**, 4062–4066.
18 X. J. Lang, W. H. Ma, Y. B. Zhao, C. C. Chen, H. W. Ji and J. C. Zhao, *Chem. – Eur. J.*, 2012, **18**, 2624–2631.
19 M. Rueping, J. Zoller, D. C. Fabry, K. Poscharny, R. M. Koenigs, T. E. Weirich and J. Mayer, *Chem. – Eur. J.*, 2012, **18**, 3478–3481.
20 D. G. Ma, Y. Yan, H. W. Ji, C. C. Chen and J. C. Zhao, *Chem. Commun.*, 2015, **51**, 17451–17454.
21 Y. Liu, M. Zhang, C.-H. Tung and Y. Wang, *ACS Catal.*, 2016, **6**, 8389–8394.
22 D. C. Fabry, Y. A. Ho, R. Zapf, W. Tremel, M. Panthofer, M. Rueping and T. H. Rehm, *Green Chem.*, 2017, **19**, 1911–1918.
23 D. Ma, A. Liu, C. Lu and C. Chen, *ACS Omega*, 2017, **2**, 4161–4172.
24 X. Qiao, S. Biswas, W. Wu, F. Zhu, C.-H. Tung and Y. Wang, *Tetrahedron*, 2018, **74**, 2421–2427.
25 J. Li, A. Liu, Y. Wang, S. Zhai, D. Ma and C. Chen, *Catal. Sci. Technol.*, 2020, **10**, 4917–4922.
26 W. Chang, C. Sun, X. Pang, H. Sheng, Y. Li, H. Ji, W. Song, C. Chen, W. Ma and J. Zhao, *Angew. Chem., Int. Ed.*, 2015, **54**, 2052–2056.
27 V. Sharma and M. S. Y. Khan, *Eur. J. Med. Chem.*, 2001, **36**, 651–658.
28 Q.-H. Li, L. Wei, X. Chen and C.-J. Wang, *Chem. Commun.*, 2013, **49**, 6277–6279.
29 W.-J. Liu, X.-H. Chen and L.-Z. Gong, *Org. Lett.*, 2008, **10**, 5357–5360.
30 N. Siemer, A. Lüken, M. Zalibera, J. Frenzel, D. Muñoz-Santiburcio, A. Savitsky, W. Lubitz, M. Muhler, D. Marx and J. Strunk, *J. Am. Chem. Soc.*, 2018, **140**, 18082–18092.
31 J. M. Coronado, A. J. Maira, J. C. Conesa, K. L. Yeung, V. Augugliaro and J. Soria, *Langmuir*, 2001, **17**, 5368–5374.
32 Y. Yan, W. Shi, Z. Yuan, S. He, D. Li, Q. Meng, H. Ji, C. Chen, W. Ma and J. Zhae, *J. Am. Chem. Soc.*, 2017, **139**, 2083–2089.